Preprints, 4th IFAC Conference on
Advances in Proportional-Integral-Derivative Control
Almería, Spain | June 12-14, 2024

PI-based Active Tower Damper for Offshore Wind Turbines

M. A. López-Romero*, M. Serrano*, J.E. Sierra-García, M. Santos*****

**Computer Science Faculty, Complutense University of Madrid, Madrid, 28040 Spain (e-mail: miglop23@ucm.es; mikeserr@ucm.es).*
***Department of Digitalization, University of Burgos, Burgos, 09006, Spain (e-mail: jesierra@ubu.es)*
**** Institute of Knowledge Technology, Complutense University of Madrid, Madrid, 28040, Spain (e-mail: msantos@ucm.es)}*

Abstract: This work presents an Active Tower Damping (ATD) control architecture that reduces the vibration of the tower of a wind turbine by regulating the pitch angle of the blades. PI regulators are applied to implement the ATD. Two different input configurations are proposed: one based on acceleration and the other on speed. The performance of both configurations is analyzed and compared in the frequency and time domains on a realistic model of a floating turbine simulated with the OpenFAST tool. The findings show how the ATD is capable of dampening the vibration amplitude and reducing the frequency response peaks of the system.

Keywords: wind turbine, active tower damping, pitch control, vibrations reduction, PID controller.

1. INTRODUCTION

The demand for wind energy has been increasing significantly over recent decades, which has driven the development and improvement of this renewable energy technology in order to reduce maintenance costs and increase efficiency (Sierra-García & Santos, 2021; Ramos-Teodoro & Rodríguez, 2022). In wind turbines, control algorithms are essential because they not only allow the expected energy production to be achieved but can also help reduce the vibrations of the wind structure, which reduces fatigue and extends the useful life of these devices. (Galán-Lavado & Santos, 2021; Zhou et al., 2023). Additionally, when vibrations decrease, lighter materials can be used, reducing construction and installation costs and simplifying operations (López-Romero & Peñas, 2023).

This twofold goal of energy efficiency and structural load reduction presents challenges from the control point of view. During the last decades, structural control (i.e., control focused on reducing oscillations) has been a very active field of study in civil engineering and its application has been extended to wind turbines, including the most complex floating offshore wind converters (FOWT) (Tian et al., 2023; Lackner & Rotea, 2011; Yang et al., 2019). Furthermore, in some cases structural control requires the application of an actuation force (active control). On the other hand, pitch actuators, which are used to adjust the angle of the blades, can be considered active actuators and can therefore be exploited to reduce vibrations. In addition, they also allow the acceleration of the top of the tower to be reduced. Since the torques experienced by a wind turbine in the fore-aft axis are substantially greater than in the side-to-side direction, this work focuses on this axis.

Structural control schemes can be classified into active, semi-active and passive control, depending on the methodology used (Tomás-Rodríguez & Santos, 2019). No external forces intervene in the passive control and their parameters are constant, so external power supply is not necessary. In semi-active control, closed-loop control algorithms adjust the coefficients of the damping device (typically springs and dampers) in response to the dynamics of the structure. In active structural control, an external force is necessary to implement the control action (Zhang et al., 2023; Nazokkar & Dezvareh, 2022).

This study presents a control architecture known as Active Tower Damping (ATD), which uses blade angle (pitch) control to reduce tower vibration. The ATD can be viewed as a controller where the reference input is zero, i.e. the vibration must be removed. Following this approach, the ATD has been implemented with PID controllers with two different input configurations, one based on the speed and another based on the acceleration of the tower top displacement (TTD). The results show how the ATD can damp vibrations, reducing their amplitude and minimizing peaks at the main frequencies system response (Serrano-Antoñanzas et al., 2023).

The rest of the paper is structured as follows. Section 2 explains how the pitch can be used to damp the tower vibrations. Section 3 describes the control architecture used to implement the ATD. The results are discussed in Section 4. The paper ends with the conclusions and future works.

2. PITCH ACTIVE TOWER DAMPING

Pitch based Active Tower Damping dampens the first mode of the fore-aft tower frequency changing the pitch angle of the blades. This pitch angle is first used to modify the surface of the blade facing the wind (Serrano et al., 2022). Wind turbines accelerate as the pitch decreases because the wind attacks a larger blade surface and vice versa, the rotor of the wind

turbines decelerates as the pitch angle increases (Sierra-Garcia et al., 2022).

The wind causes a deflection in the tower in addition to accelerating the rotor through the drag force. Normally this causes a displacement of the nacelle. Therefore, the theory underlying ATD states that as the tower moves upwind, pitch angle decreases to increase wind capture, drag force increases, and tower oscillation slows down. In contrast, pitch increases when the tower moves in the same direction as the wind, reducing wind capture, drag force, and tower speed.

Consequently, in a WT the vibrations of the nacelle can be represented quantitatively by (1):

$$F = M \cdot \ddot{x} + C(\theta) \cdot \dot{x} + K \cdot x \qquad (1)$$

where x is the displacement of the tower top (TTD) (m), $\dot{x}$ its derivative (m/s), and $\ddot{x}$ the acceleration (m/s^2). F is the drag force (N), M is the mass of the WT (kg), K is the elastic constant (N/m), and C is a function that represents the damping coefficient that depends, among other factors, on the angle of the blades, θ (º), and thus it can be adjusted by the pitch controller. Hence, by adjusting the pitch angle it is possible to act on the damping coefficient and, in turn, on the vibrations of the wind turbine (Golnary& Tse, 2022; Truong et al., 2022).

3. PI-BASED ATD CONTROL STRATEGIES

The control architecture proposed here is shown in Fig.1. The pitch controller receives the generator speed error, $GenSpd_{error}$, and generates the pitch reference, $Pitch_{ref}$. In a control without ATD this reference is used directly as input to the wind turbine. However, in this case this reference is modified by the ATD. The ATD takes into account the displacement of the nacelle, x, to generate the $ATD_{\Delta Pitch}$ signal which is added to the pitch reference to form the $Pitch_{Ref\_ATD}$ signal, which is finally used as the input of the wind turbine.

The ATD can be implemented with a PI controller. Since you want to reduce the movement of the nacelle, it is necessary to bring the speed of the nacelle or its acceleration to zero.

Therefore, one possible approach to implementing an ATD is to use a controller and set the input reference to zero. Two different PI controllers have been compared to implement the ATD. One is a PI that attempts to reduce the speed of the nacelle to zero and another is a PI that seeks to reduce to zero the tower top displacement.

The ATD output is obtained by the control law of the PI (2).

$$ATD\_\Delta Pitch = K_p \cdot e + K_I \cdot \int e \cdot dt \qquad (2)$$

where the error signal is obtained by (3) or (4), depending on the configuration of the controller.

Speed-based PI ATD:

$$e = 0 - \dot{x} \qquad (3)$$

Acceleration-based PI ATD:

$$e = 0 - \ddot{x} \qquad (4)$$

The ATD can be combined with any pitch controller. In this case, it has been combined with the pitch controller embedded in OpenFast that is also a PI controller.

The output of the pitch controller is obtained by (5-6).

$$GenSpd_{error} = GenSpd_{ref} - GenSpd \qquad (5)$$

$$Pitch_{ref} = K_p(\theta) \cdot GenSpd_{error} + K_I(\theta) \cdot \int GenSpd_{error} \cdot dt \qquad (6)$$

where $K_p(\theta)$ ·and $K_I(\theta)$ vary with the pitch angle according to equation (7), and K_p(θ = 0º) = 0.0188, K_I(θ = 0º) = 0.0080, and $\theta_k = 6.302$ º (Jonkman et al., 2009).

$$GK(\theta) = \frac{1}{1+\frac{\theta}{\theta_k}} \qquad (7)$$

Therefore, the whole architecture can be considered a two coupled PIs scheme.

4. ANALYSIS OF THE RESULTS

To validate this approach, we have used the floating offshore wind turbine NREL 5MW ITI Barge. The nominal operating conditions are rated wind speed of 11.4 m/s and nominal rotor speed of 12.1 rpm.

The reduction of vibrations of the tower has been evaluated with the following signals provided by OpenFast:

- TTDspFA [m]: Tower-top/yaw bearing fore-aft (translational) deflection (relative to the undeflected position). This signal corresponds to variable x in (1).
- YawBrTAxp [m/s^2]: Tower-top/yaw bearing fore-aft (translational) acceleration (absolute). This signal corresponds to variable $\ddot{x}$ in (1).
- TwrBsMxt [kNm]: Tower base roll (or side-to-side) moment (i.e., the moment caused by side-to-side forces).

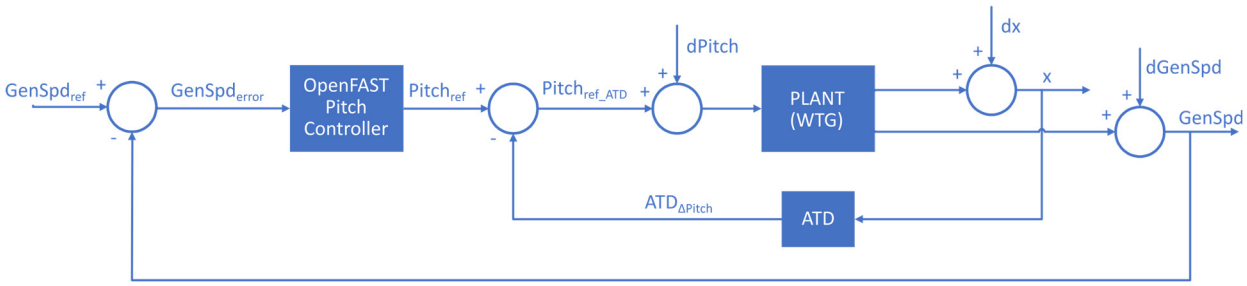

Fig. 1. ATD control architecture.

These signals are later studied in the frequency and time domain. Moreover, Fig.2 defines the different coordinates systems used by OpenFAST: turbine (t), nacelle (n), hub (h) and blade frames (b). Yawing occurs around the z_n, the rotor rotates about the x_h axis, and blade pitching occurs around the individual z_b axes.

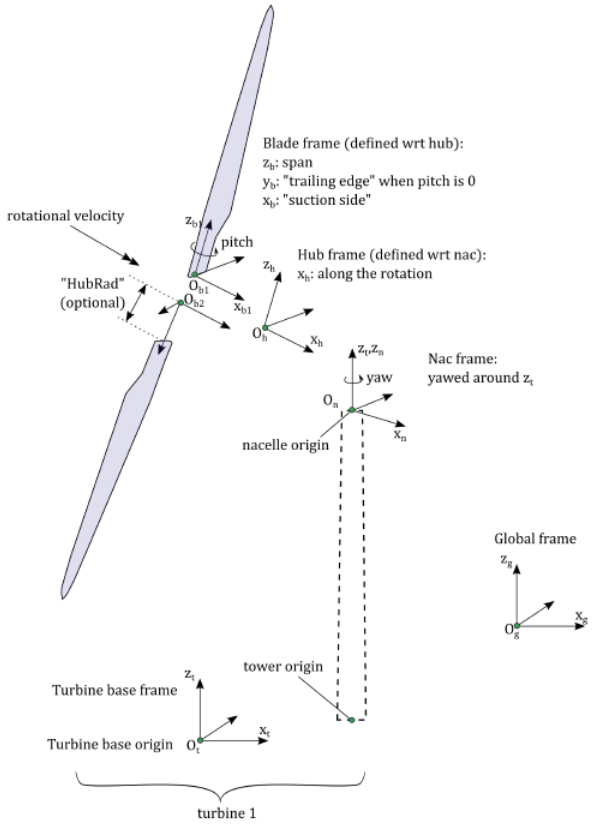

Fig. 2. System coordinates definition (NREL, 2022).

4.1 Acceleration-based PI ATD

Fig.3 shows the frequency spectrum of signals TTDspFA, YawBrTAxp, and TwrBsMxt. The blue lines indicate the results without the acceleration-based PI ATD and the red ones with the ATD. Figures 4 and 5 show a zoom at frequencies 0.6 Hz and 0.01 Hz, the most representative frequencies.

Looking at the 0.6 Hz frequency, the main peak is a little higher with the PI damper, but the frequencies around it are damped. However, the peak at 0.55 Hz has been excited. Considering the acceleration of the top of the tower, at 0.084 Hz there is also excitation, but this is not observed in the displacement of the tower top or in the tower base moment. On the other hand, the frequencies at 0.0097 Hz onwards are damped.

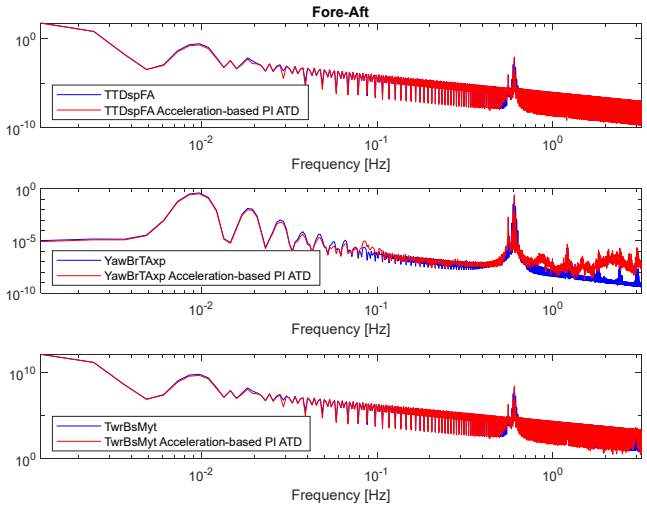

Fig. 3. Frequency spectrum of signals TTDspFA, YawBrTAxp, and TwrBsMxt with an ATD based on the tower top acceleration.

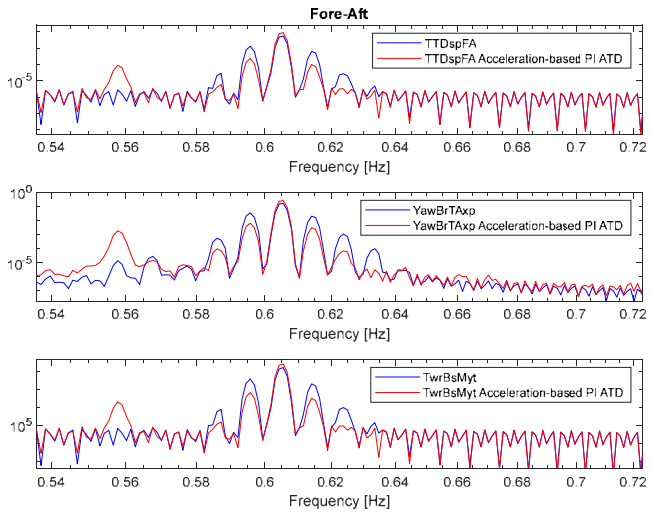

Fig. 4. Frequency spectrum of signals TTDspFA, YawBrTAxp, and TwrBsMxt with an ATD based on the tower top acceleration. Zoom at 0.6 Hz.

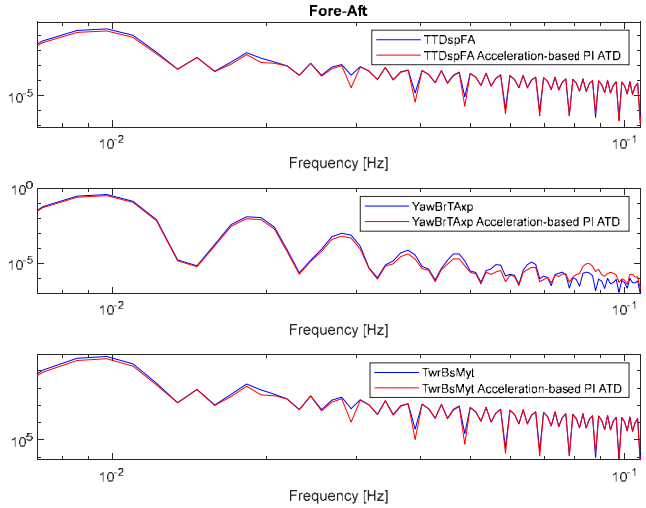

Fig. 5. Frequency spectrum of the signals TTDspFA, YawBrTAxp, and TwrBsMxt with an ATD based on the tower top acceleration. Zoom at 0.01 Hz.

Now in the time domain, Fig.6 shows the time series of the TTDspFA, YawBrTAxp and TwrBsMxt signals. The blue lines indicate the results without the acceleration-based PI ATD and the red lines when the ATD is applied. Fig.7 shows a zoom to better appreciate the details.

The gain reduction can be observed at 0.0097 Hz, where the low frequency oscillations are now smaller with the PI. In Fig.3 it can be observed that the high frequencies in the acceleration are excited with the PI. This negative effect is translated to the time domain with a noisier acceleration signal.

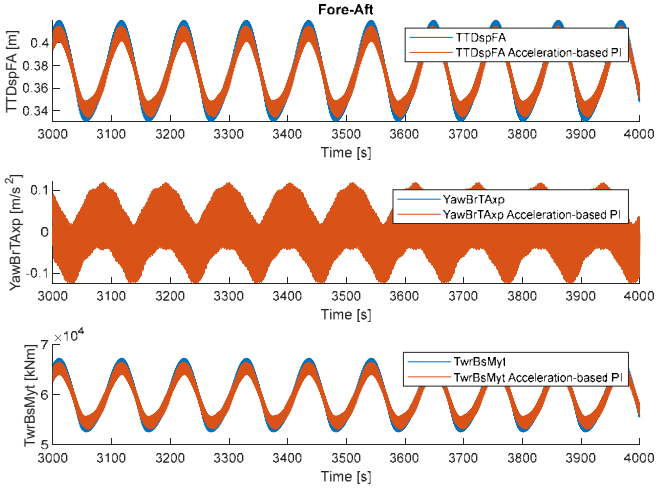

Fig. 6. Time series of the signals TTDspFA, YawBrTAxp, and TwrBsMxt with an ATD based on the tower top acceleration.

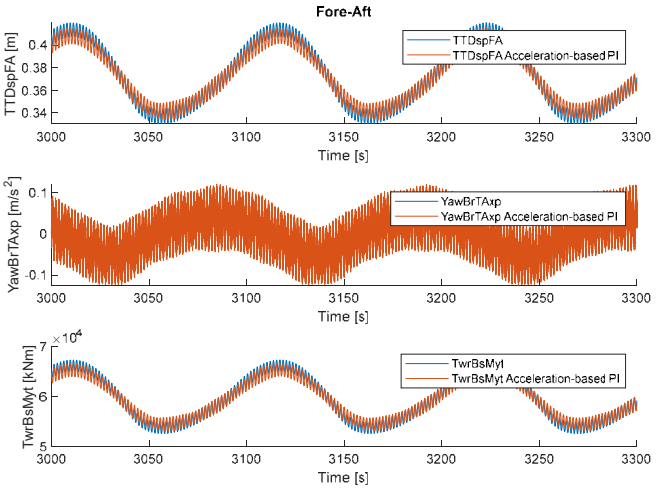

Fig. 7. Time series of the signals TTDspFA, YawBrTAxp, and TwrBsMxt with an ATD based on the tower top acceleration. Zoom.

4.2 Speed-based PI ATD

In the same way, an ATD implemented with a PI that has as input the speed of the tower top displacement has been applied. Fig.8 shows the frequency spectrum of the signals TTDspFA, YawBrTAxp, and TwrBsMxt. The blue lines indicate the results without the speed-based PI ATD and the red ones when the ATD is applied.

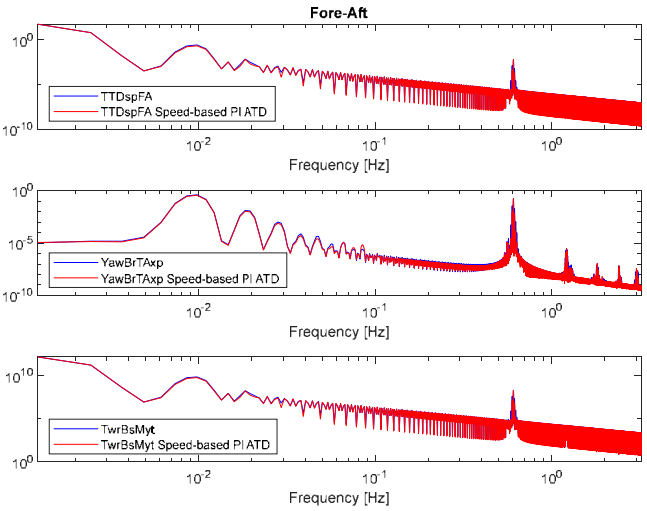

Fig. 8. Frequency spectrum of the signals TTDspFA, YawBrTAxp, and TwrBsMxt, when the tower top speed is used as input of the ATD.

Figures 9 and 10 show a zoom at frequencies 0.6 and 0.01 Hz, the most representative frequencies in the spectrum.

A damping can be observed at frequencies 0.0097 Hz and 0.6 Hz of the displacement and acceleration of the top of the tower and of the moment of the tower base. In addition, a small excitation at a frequency of 0.084 Hz can be noticed in the acceleration signal, but this negative effect is not observed in the displacement or in the base moment of the tower.

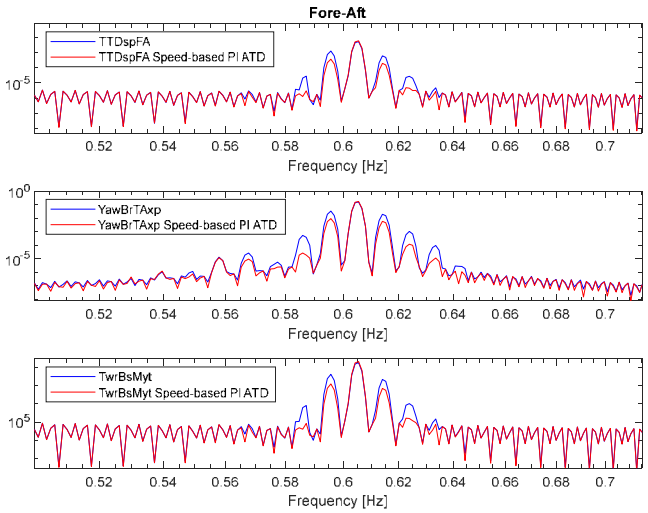

Fig. 9. Frequency spectrum of the signals TTDspFA, YawBrTAxp, and TwrBsMxt, when the tower top speed is used as input of the ATD, Zoom at 0.6 Hz.

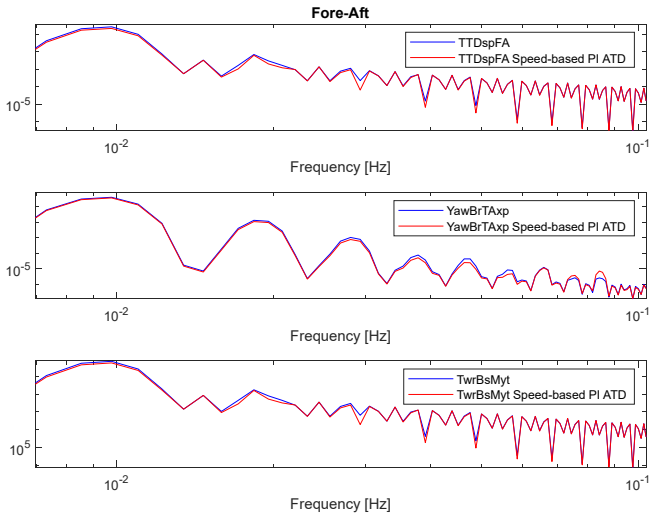

Fig. 10. Frequency spectrum of the signals TTDspFA, YawBrTAxp, and TwrBsMxt, when the tower top speed is used as input of the ATD, Zoom at 0.01 Hz.

In the time domain, Fig.11 shows the time series of the TTDspFA, YawBrTAxp and TwrBsMxt signals. The blue lines indicate the results without the speed-based PI ATD and the red lines when the ATD is applied. Fig.12 shows a zoom to better appreciate the details.

The damping observed in the power spectrum density can also be noted in the time series. The amplitude of low frequency oscillations has been reduced. This effect can be seen in the three signals studied, although the reduction is greater for TTDspFA.

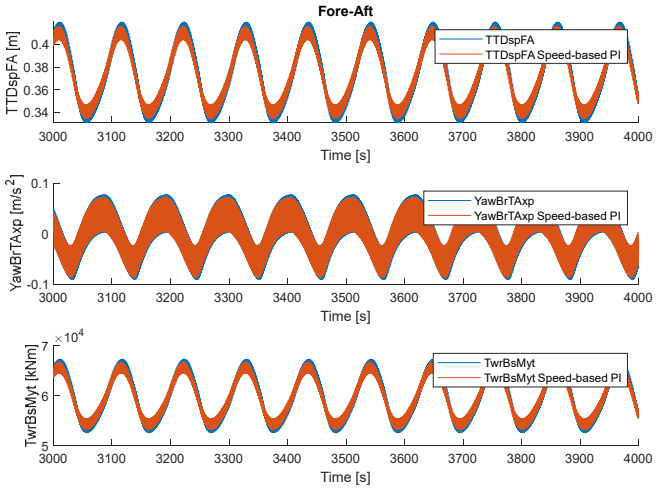

Fig. 11. Time series of the signals TTDspFA, YawBrTAxp, and TwrBsMxt, when the tower top speed is used as input of the ATD.

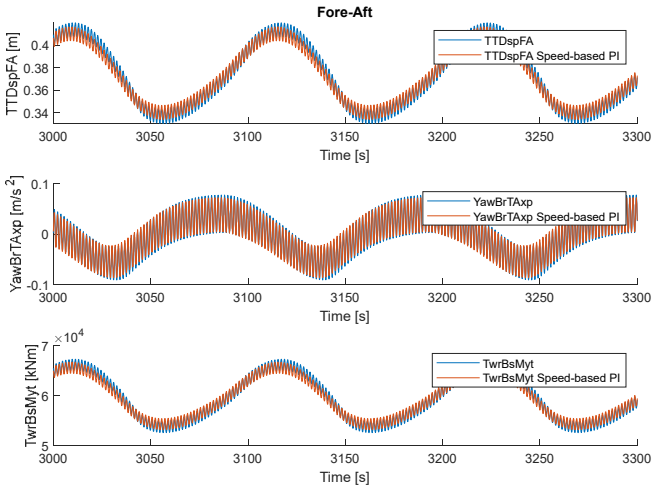

Fig. 12. Time series of the signals TTDspFA, YawBrTAxp, and TwrBsMxt, when the tower top speed is used as input of the ATD, Zoom.

4.3 Discussion of the results

Table 1 shows the comparison of the performance of the control system with the two proposed PI-based ATDs.

Table 1. Performance comparison of the PI-based ATDs

ATD input	0.01Hz	0.084 Hz	0.6 Hz	1-3Hz
Acceleration	Best damping	High excitation	Excitation at 0.55 Hz	Very High Excitation
Speed	Good damping	Little Excitation	Good Damping	No excitation

This Table 1 qualitatively shows the performance of both ATDs for the main frequency ranges, indicating for each range whether the frequencies are excited or damped.

The acceleration-based PI ATD provides greater damping for lower frequencies but at the cost of exciting the higher frequencies. On the other hand, the speed-based PI ATD

provides good damping at the lower frequencies and at the main frequency, while the rest of the frequencies are not excited or are excited very little. Therefore, the speed-based PI ATD provides the best average performance.

5. CONCLUSIONS AND FUTURE WORKS

In recent decades, there has been an unstoppable increase in wind energy due to the increase in energy demand in all countries. For energy generation to be profitable, the processes must be efficient, and in this control plays a main role. Furthermore, in the case of wind turbines, especially marine ones, it is important to prevent the structure from suffering fatigue to avoid maintenance costs and prolong its useful life.

This work proposes control systems based on conventional PID controllers that use the ATD strategy to take advantage of pitch control and actively reduce tower vibrations with the consequent improvement in turbine fatigue and the possible subsequent extension of the turbine's service life. These are some of the benefits of ATD systems, being fundamental in many wind turbines to withstand fatigue loads during their useful life.

Two configurations have been designed, with vibration speed and acceleration inputs, and in both cases the proposed control architecture allows the vibrations and their amplitude to be reduced at the relevant frequencies of the wind energy converter.

As future works, we may highlight the use of intelligent techniques to tune the PIs and it would be also desirable to validate the approach with a wind turbine prototype.

ACKNOWLEDGEMENTS

This work has been partially supported by the Spanish Ministry of Science and Innovation under the project MCI/AEI/FEDER number PID2021-123543OB-C21.

REFERENCES

Galán-Lavado, A., Santos, M. (2021). Analysis of the effects of the location of passive control devices on the platform of a floating wind turbine. *Energies*, 14(10), 2850.

Golnary, F., & Tse, K. T., (2022). Simultaneous active control of tower lateral vibration and power control of wind turbine: A novel multivariable approach. *Energy Reports*, 8, 4233-4251.

Jonkman, J., Butterfield, S., Musial, W., & Scott, G. (2009). Definition of a 5-MW reference wind turbine for offshore system development (No. NREL/TP-500-38060). National Renewable Energy Lab.(NREL), Golden, CO (United States).

Lackner, M.A., Rotea, M.A. (2011). Structural control of floating wind turbines. *Mechatronics*, 21(4), pp.704-719.

López-Romero, M. Á., & Peñas, M. S. (2023). A Positive Position Feedback controller for vibration control of wind turbines. *Energy Reports*, *9*, 1342-1353.

Nazokkar, A., & Dezvareh, R. (2022). Vibration control of floating offshore wind turbine using semi-active liquid column gas damper. *Ocean Engineering*, *265*, 112574.

Ramos-Teodoro, J. y Rodríguez, F. (2022) Producción, control y gestión distribuida de energía: una revisión de terminología y enfoques habituales, *Revista Iberoamericana de Automática e Informática industrial*, 19(3), pp. 233–253.

Serrano, C., Sierra-Garcia, J. E., & Santos, M. (2022). Hybrid optimized fuzzy pitch controller of a floating wind turbine with fatigue analysis. *Journal of Marine Science and Engineering*, *10*(11), 1769.

Serrano-Antoñanazas, M., Sierra-Garcia, J. E., Santos, M., & Tomas-Rodríguez, M. (2023). Identification of Vibration Modes in Floating Offshore Wind Turbines. *Journal of Marine Science and Engineering*, *11*(10), 1893.

Sierra-García, J.E., and Santos, M. (2021).Redes neuronales y aprendizaje por refuerzo en el control de turbinas eólicas. *Revista Iberoamericana de Automática e Informática industrial* 18.4 327-335.

Sierra-Garcia, J. E., Santos, M., & Pandit, R. (2022). Wind turbine pitch reinforcement learning control improved by PID regulator and learning observer. *Engineering Applications of Artificial Intelligence*, *111*, 104769.

Tian, H., Soltani, M. N., & Nielsen, M. E. (2023). Review of floating wind turbine damping technology. *Ocean Engineering*, *278*, 114365.

Tomás-Rodríguez, M., Santos, M. (2019). Modelling and control of floating offshore wind turbines. *Revista Iberoamericana de Automática e Informática Industrial*, 16(4) 381–390.

Truong, H. V. A., Dang, T. D., Vo, C. P., & Ahn, K. K. (2022). Active control strategies for system enhancement and load mitigation of floating offshore wind turbines: A review. *Renewable and Sustainable Energy Reviews*, *170*, 112958.

Yang, J., He, E.M. and Hu, Y.Q. (2019). Dynamic modeling and vibration suppression for an offshore wind turbine with a tuned mass damper in floating platform. *Applied Ocean Research*, 83, pp.21-29.

Zhang, H., Wen, B., Tian, X., Li, X., Dong, Y., Wang, M., & Peng, Z. (2023). Experimental study on mitigating vibration of floating offshore wind turbine using tuned mass damper. *Ocean Engineering*, *288*, 115974.

Zhou, B., Zhang, Z., Li, G., Yang, D., & Santos, M. (2023). Review of Key Technologies for Offshore Floating Wind Power Generation. *Energies*, *16*(2), 710.

National Renewable Energy Laboratory (NREL). (2022). OpenFAST Documentation. Release v3.2.0.